Structural phase transitions in the perovskite-type layer compound NH3(CH 2)5NH3CdCl4

P. Negrier, M. Couzi, N.B. Chanh, C. Hauw, A. Meresse

Classification
Physics Abstracts
61.14F — 61.50K — 63.20D — 64.70K — 78.30

Structural phase transitions in the perovskite-type layer compound $NH_3(CH_2)_5NH_3CdCl_4$

P. Negrier (1), M. Couzi (2), N. B. Chanh (1), C. Hauw (1) and A. Meresse (1)

(1) Laboratoire de Cristallographie et de Physique Cristalline, U.A.144 C.N.R.S., Université de Bordeaux I, 33405 Talence Cedex, France
(2) Laboratoire de Spectroscopie Moléculaire et Cristalline, U.A.124 C.N.R.S., Université de Bordeaux I, 33405 Talence Cedex, France

(*Reçu le 16 mai 1988, révisé le 25 octobre 1988, accepté le 25 octobre 1988*)

Résumé. — Le composé du type pérovskite feuilletée $NH_3(CH_2)_5NH_3CdCl_4$ présente deux transitions de phase structurales observées respectivement à $T_{c_1} = 337$ K et $T_2 = 417$ K. Ces transitions de phase sont étudiées par diffraction et diffusion diffuse des rayons X, ainsi que par diffusion Raman. L'existence d'un désordre conformationnel des chaînes pentylènediammonium entre des formes « trans » et « torsadées » est mise en évidence, ainsi que celle d'un désordre orientationnel de ces chaînes ; les formes « torsadées », moins stables que les formes « trans », sont thermiquement activées. La transition du deuxième ordre à T_{c_1} (Pnam ⇔ Imam) correspond à une mise en ordre dans l'orientation des chaînes « trans » ; le désordre résiduel persistant bien en dessous de T_{c_1} est attribué aux chaînes « torsadées » qui restent orientationnellement désordonnées. Le système s'ordonne progressivement à basse température, au fur et à mesure que les chaînes « torsadées » disparaissent par effet thermique. La transition du premier ordre à T_2 (Imam ⇔ C2/m) est due aux chaînes « torsadées » dont la proportion augmente avec la température ; la phase monoclinique stable au-dessus de T_2 contient uniquement des chaînes « torsadées », orientationnellement désordonnées. Une description phénoménologique de cette séquence transitionnelle est proposée, basée sur un développement de l'énergie libre de Landau, en termes de variables de pseudo-spin déterminées à partir d'un modèle de pseudo-spin multidimensionnel décrivant le désordre orientationnel des chaînes pentylènediammonium.

Abstract. — The perovskite-type layer compound $NH_3(CH_2)_5NH_3CdCl_4$ exhibits two structural phase transitions observed at $T_{c_1} = 337$ K and $T_2 = 417$ K, respectively. These phase changes are studied by means of X-ray diffraction, X-ray diffuse scattering and Raman scattering experiments. Evidence is provided for the existence of a conformational disorder of the pentylenediammonium chains between « trans » and « twisted » states, superimposed on orientational disorder ; the « twisted » states of the chains are less stable than the « trans » ones and are thermally activated. The second order transition at T_{c_1} (Pnam ⇔ Imam) is due to orientational ordering of the « trans » chains ; the residual disorder observed well below T_{c_1} is attributed to the « twisted » chains which remain orientationally disordered. The system progressively gets ordered at low temperature, as the « twisted » chains are dying out by thermal effect. The first order transition at T_2 (Imam ⇔ C2/m) is driven by an increasing proportion of « twisted » chains with increasing temperature ; the monoclinic phase stable above T_2 contains « twisted » chains only, arranged in an orientationally disordered manner. A phenomenological description of this phase sequence is proposed, based on a Landau-type development of the free energy, in terms of pseudo-spin variables derived from a multidimensional pseudo-spin model that describes orientational disorder of the pentylenediammonium chains.

1. Introduction.

Structural phase transitions in perovskite-type layer compounds have gained much interest in recent years. Many studies have been published on the substances with formula $(C_nH_{2n+1}NH_3)_2MCl_4$ (with M = Mn, Cd, Cu ...) referred to as the « monoammonium » series (see for instance Refs. [1-5] and the references cited). The structure is built up from infinite layers made of corner-sharing MCl_6 octahedra (two-dimensional perovskite type arrangement), with the alkylammonium chains in between, oriented perpendicular or nearly perpendicular to the layer planes. The NH_3 groups form NH...Cl hydrogen bonds with the octahedra, and the inter-layer bonding is achieved by means of long-range coulombic forces as well as by Van der Waals contacts between the CH_3 ends. The structural changes in these compounds are the result of reorientational motions of the alkylammonium chains, coupled to octahedron tilts occurring in the perovskite layers. In the case of long-chain compounds, additional phase transitions are observed due to a partial « melting » of the chains according to the existence of « trans »-« gauche » equilibriums and of kink motions along the chains.

Structural phase transitions have also been reported in compounds with the general formula $NH_3(CH_2)_nNH_3MCl_4$ belonging to the so-called « diammonium » series [6]. The link between adjacent octahedron planes is now achieved by the alkylene chains bearing NH_3 groups on both ends. Several structure determinations in this series have been performed [7-12] : a drastic even-odd effect in the number of carbon atoms of the diammonium chain governs the structural properties of these materials. Structural changes due to the reorientational dynamics of these chains have been evidenced [6, 11-16], but in contrast to the monoammonium series chain « melting » has not been observed, probably because of a high rigidity of the diammonium chains due to the NH...Cl hydrogen bonds at both ends. Nevertheless, conformational disorder has been found in the high temperature phases, described by an equilibrium reaction of the chains between « all-trans » and « twisted » conformations [6, 11].

The pentylenediammonium cadmium tetrachloride, $NH_3(CH_2)_5NH_3CdCl_4$ ($2C_5Cd$ for short) appears to be of special interest, since it exhibits an unusual phase sequence where the phase stable at high temperature is that of lowest symmetry [6, 17, 18] ([1]) :

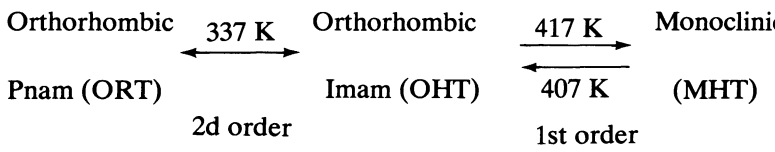

It was established that the second-order phase transition at 337 K is governed essentially by order-disorder processes due to the reorientational dynamics of the diammonium chains [6, 18]. In the orthorhombic room temperature phase (ORT) (Fig. 1), the pentylenediammonium chains are quasi-planar, and the mean planes of the chains are ordered with an angle of about 36° with respect to the **b** axis [18]. In the orthorhombic high temperature phase (OHT), the diammonium chains exhibit orientational disorder ; they are distributed between two energetically equivalent orientations, deduced from each other by the (**bc**) mirror plane. So, a rotation of about 90° around the long axis (**c** direction) brings the chains from orientation (1) to orientation (2).

([1]) For convenience, we adopt here the convention that the crystallographical **c** direction refers to the direction perpendicular to the layer planes, which coincides with the four-fold axis of a tetragonal parent phase with P4/mmm symmetry [6]. The correspondence with the standard notation for the space-groups [18] is merely obtained by exchanging the roles of the **b** and **c** directions.

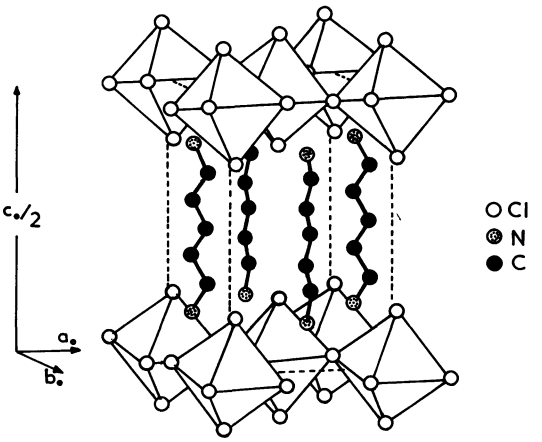

Fig. 1. — A schematic representation of the structure of $2C_5Cd$ in the ordered phase (after Ref. [18]).

A microscopic rigid-lattice model was developed in the mean field approximation, to account for the second order transition of $2C_5Cd$ at 337 K and for the similar ones occurring in $2C_3Cd$ and $2C_4Mn$; in this model, « twisted » conformations of the chains were introduced in addition to the « all-trans » conformations [6]. The « twisted » conformation corresponds to a state where the upper end of the chain has orientation (1) and the lower one orientation (2), or *vice versa*. The « twisted » chains are shorter than the all-trans ones ; also, they are less stable but they can be thermally activated. So, an increasing proportion of « twisted » chains is expected with increasing temperatures, which may account for the negative thermal expansion coefficient observed in the crystallographic **c** direction parallel to the chain axis [6, 18]. « Twisted » chains were evidenced in $2C_4Mn$ from a neutron diffraction structural determination [11], and more recently in $2C_5Cd$ from an X-ray diffraction study [18]. Their existence is further supported by the entropy change observed at the phase transition [6, 16] and by incoherent quasielastic neutron scattering data obtained with $2C_5Mn$ [19].

Thus, the transition mechanisms in these systems appear to be rather complex, due to the superposition of orientational and conformational disorders of the diammonium chains. Moreover, the structural characteristics of the monoclinic high temperature phase (MHT) observed only with $2C_5Cd$, as well as the physical processes governing the occurrence of this structural modification are completely unknown. In order to learn more on the phase transitions of $2C_5Cd$, we have undertaken extensive experimental studies including calorimetric, optical, Raman scattering, X-ray diffraction and X-ray diffuse scattering measurements. A preliminary report of this work, as well as a detailed presentation of the structure of the ORT and OHT phases have been published elsewhere [17, 18]. In this paper, we intend to give a complete analysis of all experimental results obtained with the different techniques ; a phenomenological description of the phase transitions based on a Landau development of the free energy in terms of a multidimensional pseudo-spin model will also be proposed.

2. Experimental details.

2.1 SAMPLE PREPARATION. — Colourless single crystals of $2C_5Cd$ have been grown by slow evaporation of aqueous solutions containing stoichiometric amounts of pentylenediammonium and cadmium chlorides. Small crystals about $0.2 \times 0.2 \times 0.05$ mm, as well as polycrystalline powders have been used for X-ray studies. Platelets of about $5 \times 10 \times 2$ mm

and $1 \times 1 \times 1$ mm have been used for Raman scattering and optical measurements respectively, while DTA measurements have been performed on powdered samples.

2.2 X-RAY DIFFRACTION. — Powder X-ray diffraction experiments as a function of temperature have been performed with either a Guinier-Lenné or a Guinier-Simon camera (using the CuK_α radiation obtained with a quartz monochromator). A powder SECASI counter diffractometer equipped with a home-made heating unit has also been used.

Single crystals of the ORT and OHT structural modifications have been studied with Weissemberg and precession cameras, as well as with a four-circle CAD4 diffractometer (using the MoK_α radiation obtained with a graphite monochromator). The temperature variations were achieved by means of a ENRAF-NONIUS gas flow system.

2.3 RAMAN SCATTERING. — The Raman spectra of $2C_5Cd$ single crystals have been recorded between 80 and 433 K on a CODERG T 800 triple monochromator instrument, coupled with an argon-ion laser SPECTRA-PHYSICS model 171. The emission line at 514.5 nm was used for excitation, with an incident power not exceeding 500 mW. A cooled RCA photomultiplier was used for detection. Low temperature measurements down to 80 K were made with a liquid nitrogen cryostat C3N from DILOR, and a home-made heating unit was used for measurements up to 433 K. In both cases, the temperature regulation of the sample, monitored by a thermocouple, was better than $\pm$ 0.5 K.

3. Results and discussion.

3.1 DTA EXPERIMENTS AND OPTICAL OBSERVATIONS. — Preliminary characterizations of the structural phase transitions occurring in $2C_5Cd$ have been made by DTA. Numerous cycles of heating and cooling between 110 K and 450 K always show the presence of two thermal accidents related to previously reported phase transitions [6, 16]. The first one, occurring at $T_{c_1} = 337$ K, looks like a specific heat anomaly and does not exhibit thermal hysteresis in the limit of experimental accuracy ; it is probably related to a second-order transition. The second one occurs at $T_2 = 417$ K on heating (407 K on cooling) ; it is related to a first order transition.

Observations of a $2C_5Cd$ single crystal at room temperature through a polarizing microscope confirm the orthorhombic symmetry ; extinctions are clearly seen along the three crystallographical directions denoted $\mathbf{a}_0$, $\mathbf{b}_0$ and $\mathbf{c}_0$. No change in the behaviour of the crystal is noticed at the transition at T_{c_1}, as expected for the Pnam $\Leftrightarrow$ Imam (orthorhombic-orthorhombic) transformation [6, 18]. Above T_2 strong damage occurs in the crystal, resulting in a very dense domain pattern, but the same extinctions are still noticed for observation along $\mathbf{c}_0$, which means that at least one of the indicatrix axes lies parallel to $\mathbf{a}_0$ or $\mathbf{b}_0$; in contrast, we could not detect any extinction for observation along $\mathbf{a}_0$ or $\mathbf{b}_0$. In agreement with previous conclusions [6], this behaviour can be understood by the occurrence of a monoclinic structure above T_2, with complex twinning phenomena, and with the monoclinic axis lying either along $\mathbf{a}_0$ or $\mathbf{b}_0$.

3.2 X-RAY DIFFRACTION. — A Guinier-Lenné photograph obtained with $2C_5Cd$ is shown in figure 2. A continuous evolution of the diffraction patterns is observed at $T_{c_1} = 337$ K (ORT $\Leftrightarrow$ OHT), as expected for a second-order transition ; one notices a small inflexion in the positions of the diffraction lines as a function of temperature, as well as a progressive disappearance of a number of lines when reaching the OHT phase. In contrast, the transition at $T_2 = 417$ K (OHT $\Leftrightarrow$ MHT) is characterized by abrupt changes in the diffraction patterns and by the existence of the two phases in a temperature range of ≈ 10 K around T_2 (first order transition).

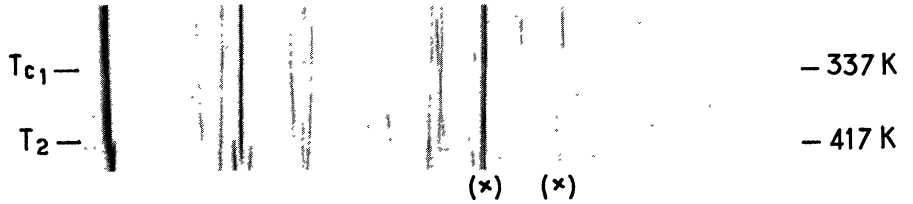

Fig. 2. — Guinier-Lenné photograph obtained with $2C_5Cd$. The reflexions due to the sample holder are noted by (×).

3.2.1 *The orthorhombic* ORT *and* OHT *phases.* — A detailed presentation of the structural determination of the ORT (Pnam) and OHT (Imam) phases has been published elsewhere [18]. In particular, the existence of orientational disorder of the chains as well as the presence of conformational disorder between « trans » and « twisted » states has been evidenced in the OHT phase, whereas the ORT phase is described essentially as an ordered structure [18]. In figure 3, we have reported the temperature evolution of the lattice parameters through the ORT ⇔ OHT transition at T_{c_1}, obtained from single crystal data (CAD4). The thermal expansion coefficient is positive along $\mathbf{a}_0$ and $\mathbf{b}_0$ but it is negative along $\mathbf{c}_0$; as already mentioned [6, 18], an increasing proportion of « twisted » chains with increasing temperature may account for the decrease of the interlayer distance. However, the unit-cell volume remains practically constant in this temperature range (Fig. 3).

The anomalies in the temperature variation of the lattice parameters observed below T_{c_1} (Fig. 3) can be explained by a coupling of the order parameter μ (see Sect. 4.1.3) with the

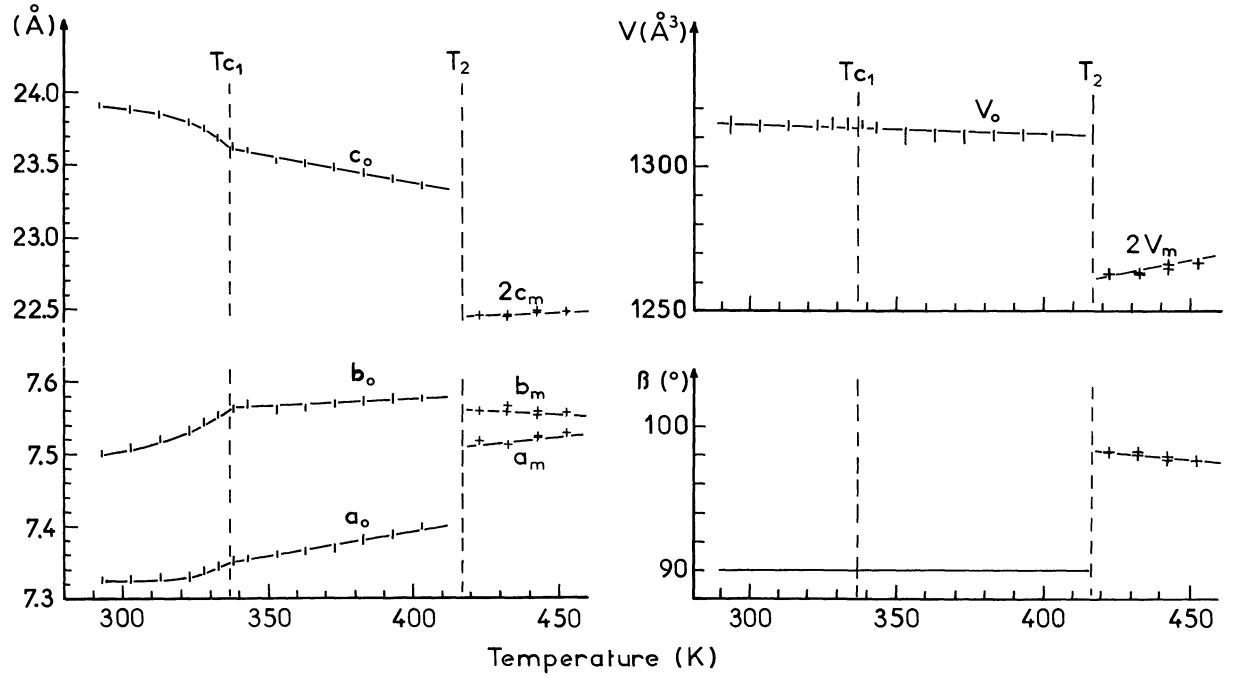

Fig. 3. — Evolution with temperature of the lattice parameters of $2C_5Cd$ in its different structural modifications. | corresponds to single crystal data ; + corresponds to power data.

volume strain components u_{ii} $(i = x, y, z)$; this coupling term should be of the form $\delta \mu^2 u_{ii}$ where δ is the coupling coefficient, so that a temperature dependence of the lattice parameters in $(T_{c_1} - T)^{2\beta}$ is expected below T_{c_1}, β being the critical exponent of the order-parameter. The experimental accuracy is not good enough to determine reliable values of β ; however, there is a clear deviation from linear variation below T_{c_1}, which means that $2\beta \ll 1$ (Fig. 3). Indeed, departure from the classical mean field behaviour ($\beta = 0.5$) has been evidenced by means of NQR experiments, which give $\beta = 0.26 \pm 0.02$ [6].

3.2.2 *The monoclinic* MHT *phase.* — We could not take advantage of single crystal data in the MHT phase, because of complex twinning phenomena. The powder diffraction diagrams obtained above T_2 reveal the splitting of several lines (Fig. 2) consistent with a monoclinic structure. Indeed, a monoclinic unit-cell can be found, with dimensions similar to those determined in the orthorhombic structural modifications, and with the unique axis lying parallel to $\mathbf{a}_0$ or $\mathbf{b}_0$ (see Sect. 3.1). The corresponding indexation shows that all observed lines have an even Miller index ℓ, which is consistent with a monoclinic parameter $c_m \approx \frac{1}{2} c_0$; furthermore, the systematic absence of lines with $h + k = 2n + 1$ suggests the existence of a base-centred monoclinic structure. It follows that the most symmetrical space-group for the MHT phase compatible with the powder diffraction patterns is C12/m1, with lattice parameters such as $a_m \approx a_0$, $b_m \approx b_0$ (monoclinic axis), $c_m \approx \frac{1}{2} c_0$ and $\beta \neq 90°$. At this point of the analysis, this choice for the space-group is not unique, but it will be justified later on (see Sect. 4.1.2).

The lattice parameters of the MHT phase have been determined after least-square refinements of the powder data, and their temperature evolution is shown in figure 3. There is an abrupt downwards shift of $2 c_m$ at T_2, and at the same time, the a_m and b_m parameters become almost equal ; the shear deformation is rather large ($\beta \approx 97°$) but it has a tendancy to decrease with increasing temperatures. As a result, the unit-cell volume, related to the same number of formula units, is smaller in the MHT phase than in the orthorhombic phases (Fig. 3), which is an unusual behaviour for a high temperature phase ; this can be explained by a predominant proportion of « twisted » chains in MHT (see Sect. 3.4.1). Since $a_m \approx b_m$, the octahedron layers must exhibit a quasi ideal chessboard like arrangement, very close to that expected for the parent structure (hereafter referred to as THT) with space-group P4/mmm [6]. Indeed, on heating, we notice a slight evolution of the lattice constants towards values ($a_m = b_m$, $\beta = 90°$) that would be expected for the THT phase (Fig. 3), but the MHT $\Leftrightarrow$ THT transition is not observed because of a chemical decomposition starting around 450 K.

3.3 X-RAY DIFFUSE SCATTERING. — From X-ray diffuse scattering experiments, it has been shown that disordering processes occurring in $(CH_3NH_3)_2CdCl_4$ (« monoammonium » series) concern not only the ammonium groups but also the $CdCl_6$ octahedron layers, because of the NH...Cl hydrogen bond interactions existing between the two sub-lattices ; in this case, it was shown that short-range correlations take place essentially in the layer planes [20].

We have performed such experiments with $2C_5Cd$ single crystals at different temperatures in the ORT and OHT phases, in order to characterize the disordering processes occurring in a crystal of the « diammonium » series, by comparison with « monoammonium » compounds. Fixed-crystal photographs have been obtained with a precession camera by using monochromatized Mo radiation (Fig. 4) ; exposure times of about 24 hours were necessary (incident power ~ 1.5 kW and crystal size $1 \times 0.8 \times 0.2$ mm) to observe the diffuse scattering patterns correctly.

3.3.1 *Room temperature data (*ORT *phase).* — As shown in figure 4a, in the reciprocal (**b*** **c***) {or (**a*** **c***)} plane, one notices the presence of well defined diffuse streaks parallel to **c*** ; they are due to diffuse reciprocal row lines and not to diffuse planes, because they completely disappear as a result of a slight misorientation of the **c*** axis out of the scattering plane. The most intense row lines are indexed [62 ℓ] {or [26 ℓ]} ; in fact, because of crystal twinning occurring in the ORT phase [18], the two types of row lines are observed simultaneously. In the reciprocal (**a*** **b***) plane (Fig. 4b), diffuse dots are observed, corresponding to the intersections of the diffuse streaks with the Ewald sphere ; crystal twinning is confirmed by the splitting of these dots.

In the asusmption that structural disorder concerns both octahedron and ammonium group sub-lattices [20], most of the observed diffuse intensity must come from the disordered inorganic layers, having regards to the large atomic scattering factors of cadmium and chlorine, compared to those of hydrogen, nitrogen and carbon atoms. Since only diffuse streaks along **c*** are observed, the disorder due to the octahedra is not random, but correlations exist in the (**ab**) plane, as a result of the two-dimensional perovskite arrangement. Let us suppose, in a first step, that no correlation between layers exists in the **c** direction. Then, a modulation of the diffuse intensity along **c*** can arise from a « molecular shape » factor only.

Following the procedure described in [20], the shape factor of an idealized perovskite layer is calculated, which yields three types of diffuse row-lines, namely $h \pm k = 4n$, $h \pm k = 4n + 2$ and $h \pm k = 2n$; the corresponding diffuse intensities are presented in figure 5. So, there exist modulations in the calculated scattered intensities extending over 9 to 10 reciprocal unit-cells along **c***. The spatial distribution of the diffuse intensity can be easily determined from this model (Fig. 6), and the agreement with the experimental data (Fig. 4) is quite satisfactory ; in particular, as observed experimentally, the model predicts predominant intensities for the [62 ℓ] or [26 ℓ] row lines, since they correspond to $h \pm k = 4n$ associated with $I_\ell^{(1)}$ (Fig. 5). Thus, we may conclude that the long modulation of the diffuse streaks along **c***, as well as their relative intensities, are related to the shape factor of the perovskite layers.

The diffuse streaks exhibit a finite width in the **a*** and **b*** directions (Fig. 4), that defines correlation lengths of about 13-15 unit-cells in the **a** and **b** directions. From a static point of view, one would say that each perovskite layer contains ordered domains involving 300 to 500 octahedra ; in fact, disordering processes are of a dynamic nature [6, 17, 19] and one has rather to consider the existence of fluctuating domains due to the correlated motions of linked octahedra out of their averaged positions.

Examination of the diffusion patterns (Fig. 4) also reveals the existence of marked spots inside each diffuse streak. It is difficult here to decide if it is an additional modulation of the diffusion, or if it is due to « thermal » spots arising from [62 ℓ] or [26 ℓ] reflexions in the vicinity of the Ewald sphere. We have examined systematically the intensities of those [62 ℓ] and [26 ℓ] reflexions, previously observed on the four-circle (CAD4) instrument [18] ; all of them are of the same order of magnitude. In contrast, only those with $\ell = 2n$ would be seen in figure 4, which gives some support to the hypothesis of a modulated diffusion. If it is actually the case, this means that weak correlations between successive layer planes will also exist. Indeed, as the observed spots are rather spread out, the correlation length along **c** cannot be precisely determined ; anyway, it cannot exceed 1 to 2 unit-cells, i.e. 2 to 4 inter-layer distances.

Thus, in contrast to compounds of the « monoammonium » series [20], octahedron fluctuations occurring in $2C_5Cd$ would be somewhat three-dimensional, probably because inter-layer coupling is achieved by the diammonium chains themselves, instead of Van der Waals contacts between CH_3 ends in the « monoammonium » compounds. We shall return to this point in section 4.2.1.

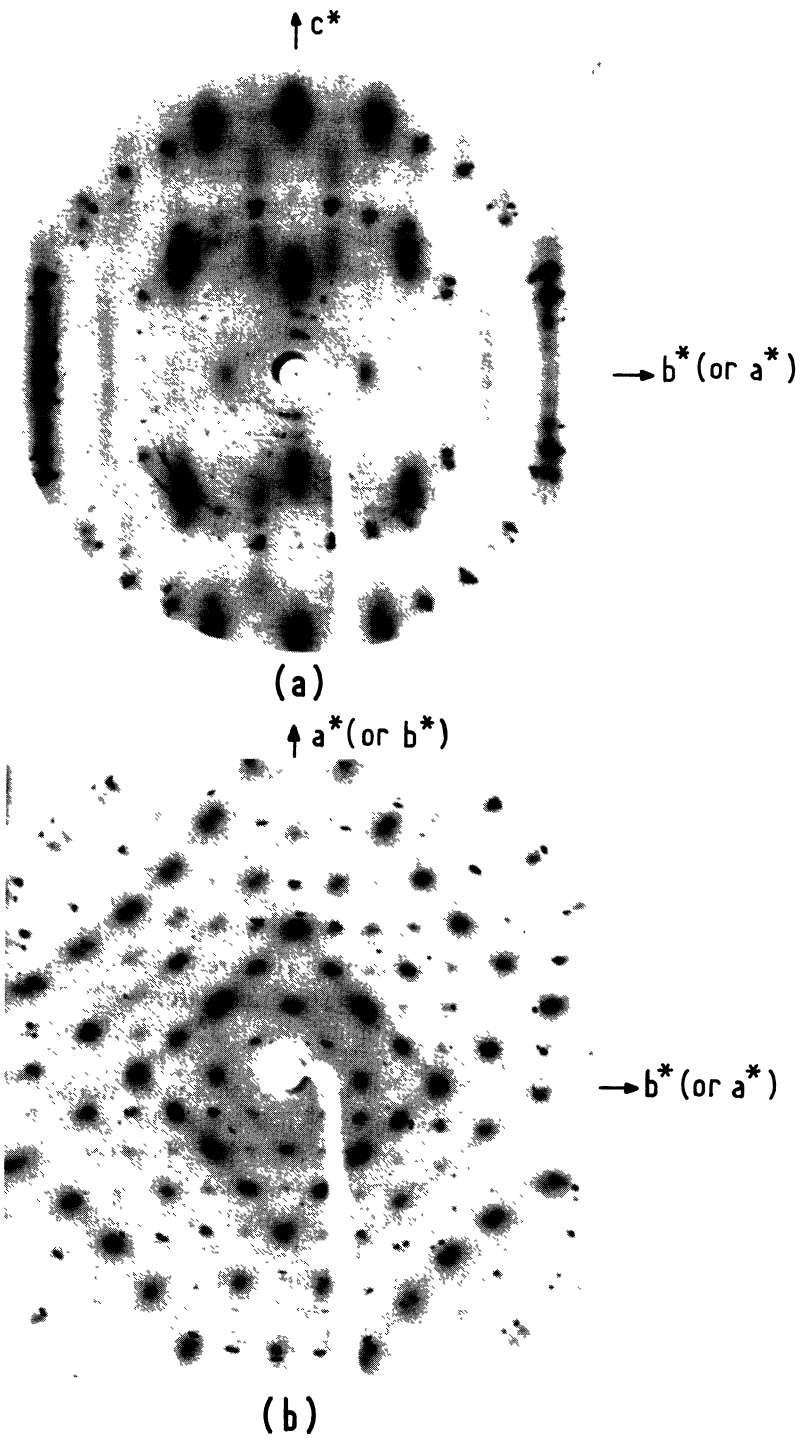

Fig. 4. — Diffuse X-ray scattering patterns observed at room temperature with $2C_5Cd$ single crystal. a) the reciprocal **a*** **c*** (or **b*** **c***) plane ; b) the reciprocal **a*** **b*** plane.

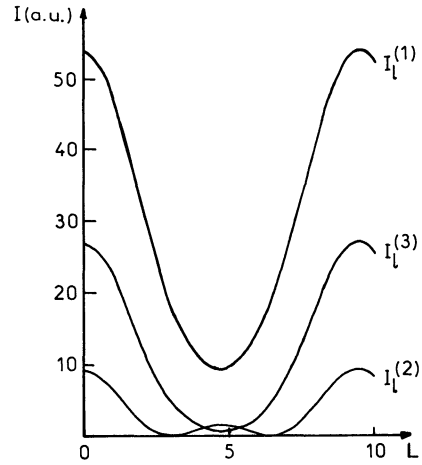

Fig. 5. — Calculated distribution of the diffuse intensity along $\mathbf{c}^*$. $I_\ell^{(i)}$ $(i = 1, 2, 3)$ correspond to $h \pm k = 4n$, $h \pm k = 4n + 2$, $h \pm k = 2n$ row lines, respectively.

3.3.2 *Temperature evolution.* — The shape of the diffuse scattering patterns is qualitatively conserved when changing the temperature. At low temperature (170 K, ORT phase) there is however a considerable decrease in the diffuse intensity as well as a marked narrowing of the diffuse streaks, indicating an increase of the correlation lengths. In contrast, at high temperature (370 K, OHT phase), one notices a decrease of the correlation lengths evidenced by the broadening of the diffuse streaks.

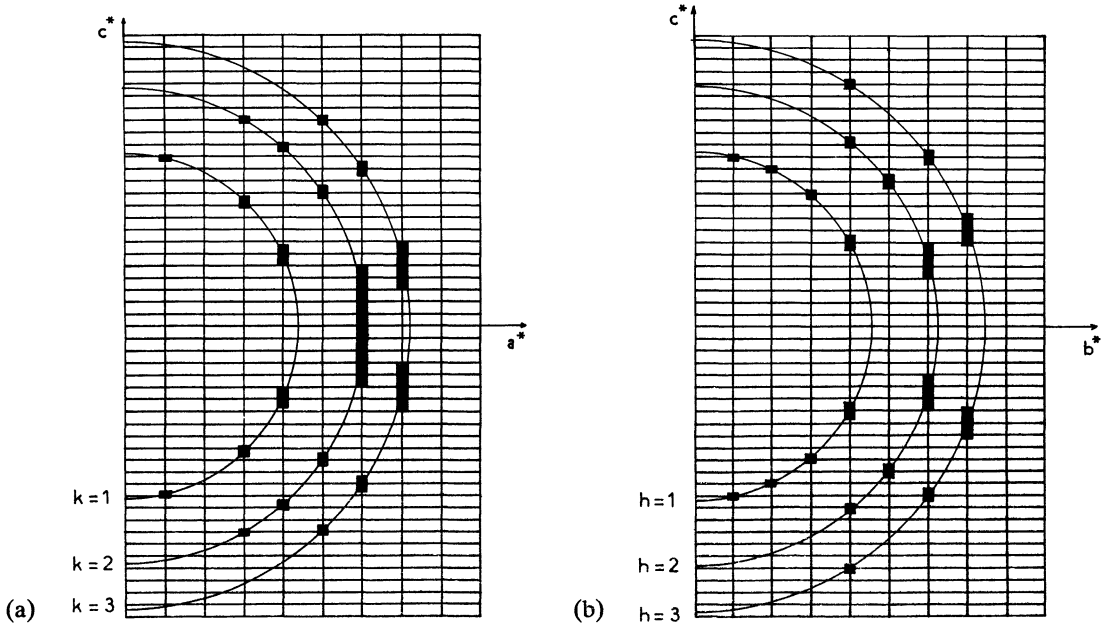

Fig. 6. — Schematic representation of the calculated spatial distribution of the diffuse intensity. a) in the reciprocal **a*** **c*** plane ; b) in the reciprocal **b*** **c*** plane ; c) in the reciprocal **a*** **b*** plane.

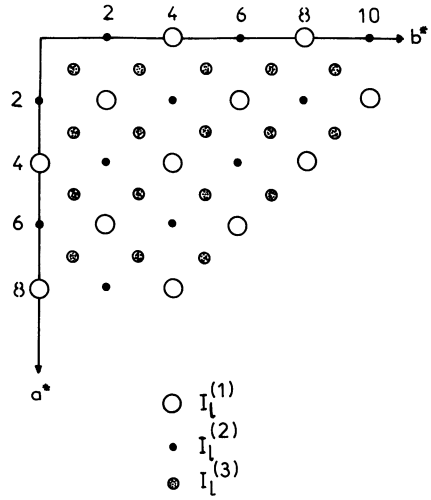

Fig. 6(c).

Further experiments including for instance a precise determination of the intensity and the width of the diffuse scattering patterns as a function of temperature, in particular near the transition point ($T_{c_1} = 337$ K), would be necessary for a more penetrating interpretation of these data in terms of rotational or translational motions of the $CdCl_6$ octahedra [21]. Nevertheless, the results up to now available, clearly show that a disordering process, due to the octahedron layers, already effective in the OHT phase, persists in the ORT phase at temperatures well below the OHT $\Leftrightarrow$ ORT transition.

3.4 RAMAN SCATTERING. — We have undertaken Raman scattering experiments on $2C_5Cd$ single crystals in order to gain information on the one hand on the conformational disorder of the pentylenediammonium chains through the study of some internal vibrational modes and on the other hand on the transition mechanisms through the study of the lattice vibrations.

3.4.1 *Internal vibrations.* — We have systematically scanned the spectra of $2C_5Cd$ between 300 and 3 400 cm^{-1}, at different temperatures ranging from 80 to 420 K. The most striking spectral changes that could be related to the existence of a conformational equilibrium of the carbon chains are observed on the $A_g(\alpha_{zz})$ spectra, in the regions of 400 to 450 cm^{-1} and of 800 to 900 cm^{-1} [22]. We do not intend to give here the complete assignments of these spectra, but as an example, we shall discuss the behaviour of a bending vibration of the NCCC backbone (accordion mode) located around 420 cm^{-1} (Fig. 7). At low temperatures ($T < 200$ K), a single line is observed at 440 cm^{-1}, assigned to the chains of « all-trans » conformation ; a new line at 420 cm^{-1} progressively grows in intensity with increasing temperature, to the expense of the « trans » line at 440 cm^{-1}. This gives rise to a continuous spectral evolution through the ORT $\Leftrightarrow$ OHT phase transition at $T_{c_1} = 337$ K, but an abrupt change is noticed at the OHT $\Leftrightarrow$ MHT transition at $T_2 = 417$ K ; in the MHT phase a broadened signal is still present at ≈ 420 cm^{-1} and the « trans » line at 440 cm^{-1} can no longer be detected (Fig. 7). The new line at 420 cm^{-1} has to be assigned to a thermally activated conformation which, in view of previous studies [6, 11], could be identified as a « twisted » conformation. We shall now develop arguments in favour of this interpretation.

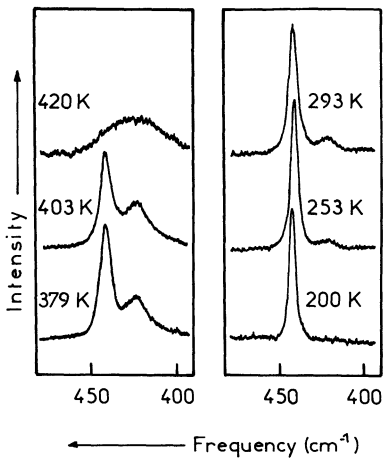

Fig. 7. — Evolution with temperature of the α_{zz} Raman spectrum of $2C_5Cd$ in the region of a CCN-CCC bending vibration.

Let us consider an equilibrium between two isolated conformers 1 and 2 (supposed in our case to be the « trans » and « twisted » forms, respectively) ; the enthalpy of the reaction $1 \Rightarrow 2$ at constant pressure is related to the equilibrium constant K through the Van't Hoff equation :

$$[\partial(\mathrm{Ln}\, K)/\partial T]_p = \Delta H/RT^2 \tag{1}$$

and if p designates the proportion of « twisted » chains, the equilibrium constant is written :

$$K = p/(1-p)\,. \tag{2}$$

Let us call $I_{1,i}$ the integrated intensity of a Raman line associated with a « trans » chain ; it concerns for example the Raman line at $\omega_i = 440\ \mathrm{cm}^{-1}$ (Fig. 7). Then we have :

$$I_{1,i} = A\,.\,[n(\omega_i)+1]\,.\,[S_{1,i}]^2\,.\,(1-p) \tag{3}$$

where $n(\omega_i) = [\exp(\hbar\omega_i/kT)-1]^{-1}$ is the Bose-Einstein population factor, $S_{1,i}$ is the Raman tensor element associated with the mode i of conformer 1, and A a constant depending on the experimental conditions. The « reduced » intensity $I^*_{1,i}$ is defined as :

$$I^*_{1,i} = I_{1,i}/[n(\omega_i)+1] = A\,.\,[S_{1,i}]^2\,.\,(1-p)\,. \tag{4}$$

Similarly, we can define for the « twisted » chains :

$$I_{2,j} = A\,.\,[n(\omega_j)+1]\,.\,[S_{2,j}]^2\,.\,p \tag{5}$$

$$I^*_{2,j} = A\,.\,[S_{2,j}]^2\,.\,p \tag{6}$$

where $I_{2,j}$ concerns for instance the intensity of the Raman line at $\omega_j = 420\ \mathrm{cm}^{-1}$ (Fig. 7). In the hypothesis where $S_{1,i}$ and $S_{2,j}$ are not temperature dependent, the equilibrium constant can be expressed as

$$K = B\,.\,(I^*_{2,j}/I^*_{1,i}) \tag{7}$$

where $B = [S_{1,i}]^2/[S_{2,j}]^2$ is a constant.

If the preceding equations are verified, the curves -Ln $(I^*_{2,i}/I^*_{1,i}) = f(1/T)$ must represent straight lines with a slope equal to ΔH. As shown in figure 8, a linear relation is indeed obtained in the ORT and OHT phases when -Ln $(I^*_{2,420\,cm^{-1}}/I^*_{1,440\,cm^{-1}})$ is plotted against $1/T$; the corresponding value for ΔH is 17.1 ± 2 kJ.mole^{-1}. Within the limit of experimental errors, the same value of ΔH can be determined from the temperature evolution of all other lines assigned to conformer 2 [22], as expected. On the other hand, similar results on chain conformational disorder have been obtained for a number of crystals in this family, namely $2C_5Mn$, $2C_4Mn$ and $2C_3Cd$ [23]. Values of ΔH in the range of 17 kJ.mole^{-1} are always found for the compounds with $n = 5$ carbon atoms but higher values are determined as the carbon chain becomes shorter, i.e. $\Delta H \approx 21$ kJ.mole^{-1} for $2C_4Mn$ and $\Delta H \approx 24$ kJ.mole^{-1} for $2C_3Cd$ [23].

Thus, the following conclusions can be drawn :

a) conformational disorder of the diammonium chains is a common characteristics of most of the compounds in this family [6] ;

b) the values of ΔH for the equilibrium reaction in between the two conformers is approximately an order of magnitude higher than the enthalpy corresponding to a « trans » $\Leftrightarrow$ « gauche » equilibrium in carbon chains [24] ; this is a strong argument in favour of the assignment of the new lines to a « twisted » conformation, since the latter is expected to be much less stable than a « gauche » form [6] ;

c) the increasing values of ΔH with decreasing lengths of the chains are more consistent with a model of « twisted » chains (where the twist angle between two neighbouring carbons is nearly constant along a chain [18] but depends on the chain length) than with a twist angle

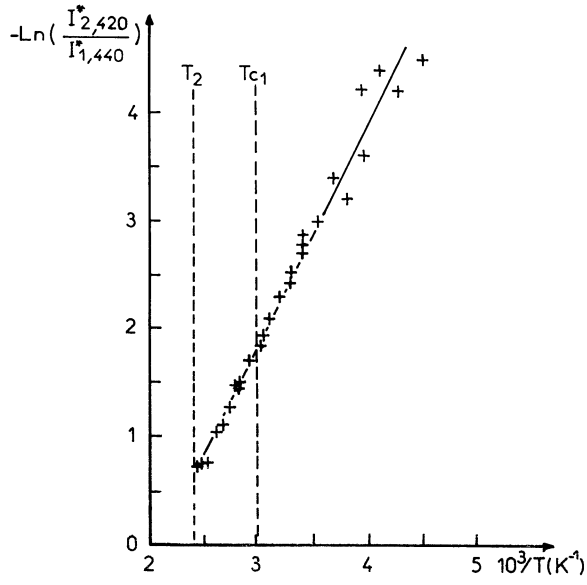

Fig. 8. — Evolution with temperature of the ratio of the reduced intensities of Raman lines at 420 cm^{-1} (« twisted » chains) and at 440 cm^{-1} (« trans » chains).

localised mainly around one particular C-C bond [11] ; as a matter of fact, in the latter case values of ΔH are not expected to vary strongly as a function of the chain length ;

d) the conformational equilibrium between « trans » and « twisted » states of the chains is apparently not modified at the ORT $\Leftrightarrow$ OHT transition (Fig. 8), but it is abruptly displaced in favour of the « twisted » conformations in the MHT phase (Fig. 7) ; in agreement with this observation, we have already noticed that the lattice parameter **c** corresponding to the chain axis exhibits an abrupt downwards shift in the MHT phase (Fig. 3), because the « twisted » chains are significantly shorter than the « trans » ones [18] ;

e) the observation of two lines separated by $20\ cm^{-1}$ and assigned to two different conformers in the ORT and OHT phases (Fig. 7) gives an estimate of a minimum life-time of these conformers of about 0.3×10^{-12} s ; now, the transformation of a « trans » conformer into a « twisted » one occurs after a reorientation by $\approx 90°$ of one NH_3 end with respect to the other one. It follows that the correlation times of NH_3 reorientational motions must be larger than 0.3×10^{-12} s, which is in accordance with experimental values (1 to 2×10^{-12} s) found in $2C_3Mn$ and $2C_5Mn$ [19, 25] ;

f) from equations (1) and (2) and with the help of experimental values $\Delta H = 17 \pm 2\ kJ.mole^{-1}$ and $p = 0.45 \pm 0.5$ at 353 K [18], the proportion p of « twisted » chains can be determined at any temperature in the ORT and OHT phases ; this gives in particular $p \approx 0.4$ at $T_{c_1} = 337$ K and $p \approx 0.7$ just below T_2.

In fact, the entropy change at T_{c_1} measured in $2C_5Cd$ [16] and $2C_5Mn$ [26] indicates a proportion of « twisted » chains significantly lower. Furthermore, as long as the « trans » and « twisted » chains in the OHT phase are constrained to be distributed between two mirror-related orientations respectively [18], the excess entropy arising from disorder

$$S_{ex} = -R\left[(1-p)\,\mathrm{Ln}\,\frac{1}{2}(1-p) + p\,\mathrm{Ln}\,\frac{1}{2}p\right]$$

would be maximum for $p = 0.5$; this condition, however, is not imposed by symmetry (see Sect. 4.2.1). Nevertheless, the value of $p = 0.45$ at 353 K [18] is probably overestimated, due to a possible artefact in the structure refinement which was performed on the basis of an idealized « twisted » chain model.

3.4.2 *Lattice vibrations.* — The so-called « lattice vibrations » of $2C_5Cd$ are due to the vibrational modes of the $CdCl_6$ octahedron layers, and to the « external » (translatory and rotatory) vibrations of the pentylenediammonium group (A^{2+}) ; they are expected to be in the range of 0 to $300\ cm^{-1}$ [27-29]. The enumeration of the Raman active lattice vibrations in the different structural modifications of $2C_5Cd$ determined from group-theoretical considerations (factor group analysis) is given in table I, along with an approximate description of these modes obtained with the help of projection operators. It should be pointed out that this analysis is based on the « averaged » structures, obtained by considering the A^{2+} groups as rigid bodies having the required site symmetry ; the disordering processes which have not been taken into account with such a procedure may result in a breakdown in the $\mathbf{q} = 0$ selection rules [28], so that a weighted one-phonon density of states (broad spectra) may be observed, superimposed on the « allowed » $\mathbf{q} = 0$ modes enumerated in table I. Of course, this enumeration is absolutely rigorous at low temperatures, when the ORT phase becomes ordered.

The low frequency Raman spectra of $2C_5Cd$ single crystal have been recorded at different temperatures by using different scattering geometries allowing the observation of all Raman

Table I. — *The Raman active lattice vibrations in the different structural modifications of* $2C_5Cd$, *according to the « averaged » structures.*

Lattice modes		ORT phase (Pnam)				OHT phase (Imam)				MHT phase (C12/m 1)	
		A_g	B_{1g}	B_{2g}	B_{3g}	A_g	B_{1g}	B_{2g}	B_{3g}	A_g	B_g
Cd-Cl_{ax} stretching		1	1	1	1	1	0	0	1	1	0
Cd-Cl_{eq} stretching		1	1	1	1	0	0	1	1	0	0
Cl_{ax}-Cd-Cl_{eq} bending		2	2	2	2	1	1	1	1	1	1
Cl_{eq}-Cd-Cl_{eq} bending		0	1	0	1	0	0	0	1	0	0
$CdCl_6$ "rotations"	R_x	1	0	1	0	1	0	0	0	0	0
	R_y	0	1	0	1	0	1	0	0	0	0
	R_z	1	0	1	0	0	0	1	0	0	0
A^{2+} translatory	T_x	1	1	0	0	0	1	0	0	0	0
	T_y	1	1	0	0	1	0	0	0	0	0
	T_z	0	0	1	1	0	0	0	1	0	0
A^{2+} rotatory	R_x	0	0	1	1	0	0	0	1	0	1
	R_y	0	0	1	1	0	0	1	0	1	0
	R_z	1	1	0	0	0	1	0	0	0	1

tensor elements. In the orthorhombic ORT and OHT phases, these tensors are of the form [30] :

$$A_g : \begin{vmatrix} a & o & o \\ o & b & o \\ o & o & c \end{vmatrix} \quad B_{1g} : \begin{vmatrix} o & d & o \\ d & o & o \\ o & o & o \end{vmatrix} \quad B_{2g} : \begin{vmatrix} o & o & e \\ o & o & o \\ e & o & o \end{vmatrix} \quad B_{3g} : \begin{vmatrix} o & o & o \\ o & o & f \\ o & f & o \end{vmatrix} .$$

It should be recalled that crystals of $2C_5Cd$ in the ORT and OHT phases exhibit a twin domain structure, where the $\mathbf{a}_0$ and $\mathbf{b}_0$ directions are exchanged between domains [18]. Now, the spectra observed at room temperature (Fig. 9) correspond to a single domain part of the crystal (selected by moving the incident laser beam at the inside of the crystal), as evidenced by the strong contrasts between the α_{xz} and α_{yz} spectra ; however, there is still an indetermination in the attribution of these spectra to B_{2g} or B_{3g} symmetry, because it is not possible to assign the $\mathbf{a}_0$ and $\mathbf{b}_0$ directions in the selected domain. The evolutions with temperature of the $A_g(\alpha_{xx}$ and $\alpha_{zz})$ and $B_{1g}(\alpha_{xy})$ spectra are shown in figures 10 to 12.

The spectra of the ORT phase at room temperature (Fig. 9) exhibit broad lines, which are further broadened in the OHT phase, but undergo considerable narrowing at low temperatures (Figs. 10-12). The continuous spectral evolution observed at the ORT $\Leftrightarrow$ OHT transition ($T_{c_1} = 337$ K) confirms the second-order character of this transformation ; on the other hand, the evolution of band widths is consistent with a progressive ordering of the system occurring on cooling, and with the remaining residual disorder in the ORT phase well below T_{c_1}. This observation fits nicely the X-ray diffuse scattering results (see Sect. 3.3). Abrupt changes in these spectra are noticed at the OHT $\Leftrightarrow$ MHT transition at $T_2 = 417$ K (first-order transition) ; as already mentioned strong damage occurs to the crystal when

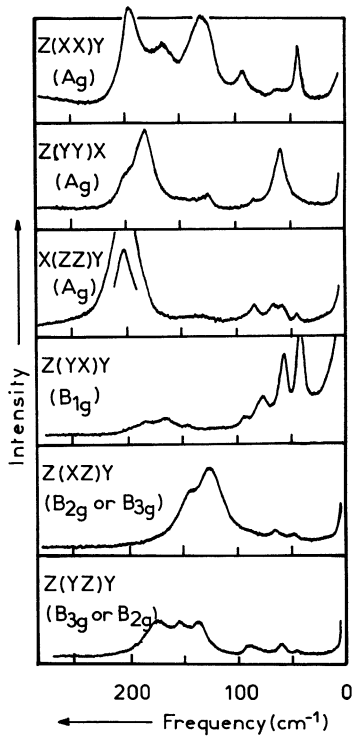

Fig. 9. — The low frequency Raman spectra of $2C_5Cd$ single crystal at room temperature.

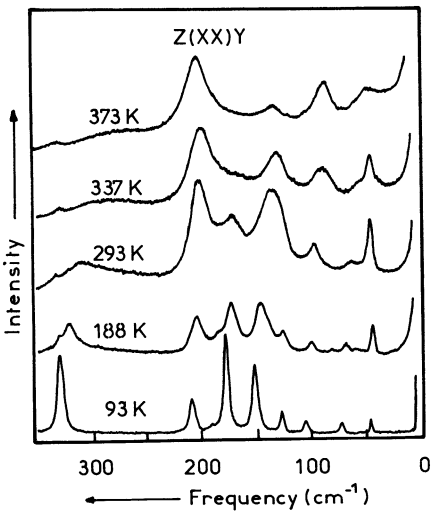

Fig. 10.

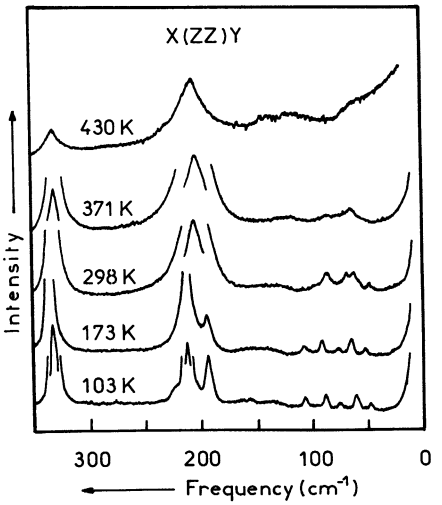

Fig. 11.

Fig. 10. — Evolution with temperature of the α_{xx} Raman spectrum of $2C_5Cd$ (low frequency part).

Fig. 11. — Evolution with temperature of the α_{zz} Raman spectrum of $2C_5Cd$ (low frequency part).

reaching the MHT phase, so that polarization selections are no longer observed : all spectra become similar to that represented in figure 11 (430 K). Nevertheless, the very broad lines observed clearly indicate that MHT is a disordered phase.

The precise assignment of these spectra is not straightforward, because a number of low lying internal modes of the pentylenediammonium chains are expected in this frequency range, in addition to the lattice vibrations. So, the strong line at 330 cm^{-1} (Fig. 11) is due to a

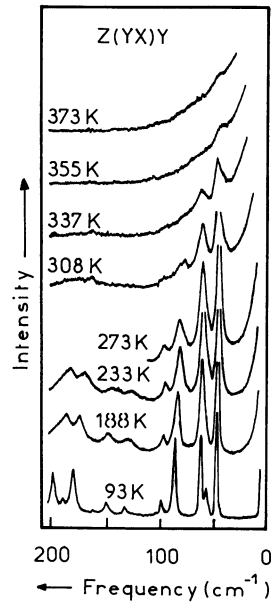

Fig. 12. — Evolution with temperature of the α_{xy} Raman spectrum of $2C_5Cd$ (low frequency part).

skeletal CCC or CCN bending mode, and that at 326 cm^{-1} (Fig. 10), which is shifted down to 240 cm^{-1} in $ND_3(CH_2)_5ND_3CdCl_4$, must be assigned to a torsional oscillation of the NH_3 group $\{\tau(NH_3)\}$. The large broadening of this line, together with the significant downwards shift of its frequency noticed on heating (Fig. 10) confirms that the NH_3 ends are directly involved in the disordering processes [29]. Another internal mode is observed at 205 cm^{-1} on the A_g spectra (Fig. 10), assigned to a Γ(CCCN) or Γ(CCCC) torsional mode of the chain ; it considerably broadens and grows in intensity with increasing temperature (Fig. 10) : this phenomenon is probably related to the « trans » $\Leftrightarrow$ « twisted » equilibrium of the chains. Then, the remaining lines are assigned to the lattice vibrations ; in the ORT phase at low temperatures, they agree with the theoretical enumeration given in table I : the Cd-Cl stretching modes are observed around 180-200 cm^{-1}, the Cl-Cd-Cl bending modes around 150 cm^{-1} and the A^{2+} external modes as well as the $CdCl_6$ « rotations » are observed at low frequency, between 0 and 120 cm^{-1} [27, 28]. It should also be pointed out that a number of lattice modes progressively disappear at the ORT $\Leftrightarrow$ OHT transition (Figs. 10-12) ; they correspond to the $\mathbf{q} = 0$ Raman active modes of the ORT phase which become zone-boundary modes in OHT (the OHT primitive unit-cell contains $Z = 2$ formula units instead of $Z = 4$ in ORT) and so become first-order optically inactive. The primitive unit-cell of the MHT phase inferred from the X-ray data (see Sect. 3.2) contains only one formula unit, which further reduces the number of allowed modes (Tab. I) ; the general trend of the

spectrum of the MHT phase obtained from a polycrystalline-like sample (Fig. 11) is in qualitative agreement with this description.

The B_{1g} (α_{xy}) spectra of the ORT and OHT phases are characterized by a « Rayleigh wing » signal whose intensity is strongly temperature dependent (Fig. 12). This signal is completely absent at low temperatures (93 K) ; it begins to appear around 200 K and grows progressively with increasing temperature while in the same time the other lines of the spectrum broaden and soften off almost completely in the OHT phase. Similar « Rayleigh wing » signals have also been observed in compounds of the monoammonium series, and they have been interpreted as diffusive like excitations due to octahedron reorientations probably coupled to the reorientational motions of the ammonium groups [28]. Such an explanation finds strong support in $2C_5Cd$ too. As a matter of fact, as far as the octahedron rotations are concerned, it can be shown from group theoretical considerations that the ORT ⇔ OHT transition is related to the « condensation » of rotations around the $\mathbf{c}_0$ axis [22] and this is further verified by the experimental data [18] ; similarly, it can be shown that rotations around the $\mathbf{a}_0$ axis have already condensed in the OHT phase [18, 22]. Then, it follows that only the rotations around the $\mathbf{b}_0$ axis are expected to generate disorder in both the OHT and ORT phases. Now, the « Rayleigh wing » signal is present only on the $B_{1g}(\alpha_{xy})$ spectrum which indeed corresponds in both phases to the symmetry of octahedron « rotations » around $\mathbf{b}_0$ (R_y rotations) and of A^{2+} reorientations around the long axis (R_z rotatory ; see Tab. I).

To summarize, the main features of the low frequency Raman spectra due to the lattice vibrations can be accounted for by the $\mathbf{q} = 0$ selection rules derived from the « averaged » structures. The disordering processes give rise to a strong broadening of these modes and to the appearance of a « Rayleigh wing » (diffusive excitations) above ≈ 200 K. Clearly, MHT is a disordered phase, and residual disorder persists in the ORT phase, at temperatures well below T_{c_1}.

4. Phenomenological analysis of the phase sequence in $2C_5Cd$.

The experimental results presented in the preceding sections, along with the structural data obtained previously [18] make it possible to develop a phenomenological analysis of the phase sequence observed in $2C_5Cd$, based on a Landau type expansion of the free-energy in terms of multidimensional pseudo-spin variables that describe the orientational disorder of the pentylenediammonium chains [31].

4.1 GROUP TO SUB-GROUP RELATIONS AND FREE-ENERGY DEVELOPMENTS. — The basic idea in this approach is to consider that all observed structural modifications of $2C_5Cd$ are derived from a tetragonal parent phase (THT), with space-group P4/mmm-D^1_{4h} ($Z = 1$) [6] and lattice parameters defined as $\mathbf{a}_t = \mathbf{b}_t \neq \mathbf{c}_t$. As already mentioned, this parent phase cannot be observed because of the chemical decomposition of the sample (see Sect. 3.2.2) ; thus, fictitious transitions THT ⇔ OHT and THT ⇔ MHT must be considered in addition to the observed ones (MHT ⇔ OHT and OHT ⇔ ORT).

4.1.1 *The* THT ⇔ OHT *transition.* — The lattice parameters a_0, b_0, c_0 of the conventional body-centred OHT unit-cell are related to those of THT by $a_0 \approx a_t\sqrt{2}$, $b_0 \approx a_t\sqrt{2}$, $c_0 = 2\,c_t$. It follows that the THT ⇔ OHT transition is driven by a lattice instability occurring at point $A(\pi/a_t, \pi/b_t, \pi/c_t)$, of the THT Brillouin zone, whose symmetry is D_{4h} [32]. All the unidimensional representations of the D_{4h} wave-vector group conserve the tetragonal symmetry, whereas the two-dimensional A_5^+/E_g and A_5^-/E_u representations lead to orthorhombic symmetry ; by taking the origin of symmetry operations at the centre of mass of

the diammonium chains, it can be easily shown by group theory that the Imam (or equivalently Ibmm) space-group is induced by A_5^-/E_u. So, the order parameter η of this transition has two components denoted by η_1 and η_2. In addition to the A_5^-/E_u representation, Γ_4^+/B_{2g} also leads to the unity representation of the OHT space-groups ; Γ_4^+/B_{2g} is associated with a secondary order-parameter denoted by ν. This transition fulfils all the Landau requirements allowing second order transformations, so that the free-energy developed in terms of primary and secondary order parameter components is of the form :

$$\Delta\Phi_1 = A_1(T - T'_{c_1})(\eta_1^2 + \eta_2^2) + C_1(\eta_1^2 + \eta_2^2)^2 + D_1(\eta_1^4 + \eta_2^4) + E_1\,\nu^2 + F_1\,\eta_1\,\eta_2\,\nu + \cdots \tag{8}$$

where T'_{c_1} is the temperature of the fictitious THT $\Leftrightarrow$ OHT transition.

Below T'_{c_1}, the solutions corresponding to the OHT phase are of the form :

$$\begin{aligned} &\eta_1 + \eta_2 \neq 0 \quad \text{with} \quad \eta_1 - \eta_2 = 0 \quad \text{(Imam)} \\ &\eta_1 + \eta_2 = 0 \quad \text{with} \quad \eta_1 - \eta_2 \neq 0 \quad \text{(Ibmm)} . \end{aligned} \tag{9}$$

These two sets of energetically equivalent solutions account for the domain structure of the OHT phase [18]. The order parameter is then $\eta = 1/\sqrt{2}(\eta_1 \pm \eta_2)$ and in this case, the free-energy can be expressed as :

$$\Delta\Phi_1 = A_1(T - T'_{c_1})\,\eta^2 + \left(C_1 + \frac{1}{2}D_1\right)\eta^4 + E_1\,\nu^2 + \frac{1}{2}F_1\,\eta^2\,\nu + \cdots . \tag{10}$$

4.1.2 *The* THT $\Leftrightarrow$ MHT *transition.* — First, we have to confirm the space group inferred for the MHT phase from X-ray powder experiments (see Sect. 3.2.2). These experiments have shown that the MHT unit-cell is base-centred monoclinic, with lattice parameters such as $a_m \approx a_0 \approx a_t\sqrt{2}$, $b_m \approx b_0 \approx b_t\sqrt{2}$ and $c_m \approx \frac{1}{2}c_0 \approx c_t$, and with the unique axis lying parallel to $\mathbf{a}_0$ or $\mathbf{b}_0$, i.e. along one two-fold diagonal axis of THT. From group theoretical considerations, it is shown that such a unit-cell is generated from THT by a lattice instability occurring at the centre of the Brillouin zone (Γ point), driven by the Γ_5^+/E_g representation ; the resulting space-group for MHT is now uniquely determined as C12/m1 (or equivalently C2/m 11), which is consistent with the diffraction patterns. So, the order parameter ρ for the THT$\Leftrightarrow$ MHT transition has two components denoted by ρ_1 and ρ_2. Again, the Γ_4^+/B_{2g} representation of the P4/mmm space-group is associated with a secondary order parameter ν, so that the relevant free-energy for this transition can be expressed as :

$$\Delta\Phi_2 = A_2(T - T'_{c_2})(\rho_1^2 + \rho_2^2) + C_2(\rho_1^2 + \rho_2^2)^2 + D_2(\rho_1^4 + \rho_2^4) + E_2\,\nu^2 + F_2\,\rho_1\,\rho_2\,\nu + \cdots \tag{11}$$

where T'_{c_2} designates the fictitious THT $\Leftrightarrow$ MHT transition temperature.

As in the preceding case, the solutions corresponding to the MHT phase are of the form :

$$\begin{aligned} &\rho_1 + \rho_2 \neq 0 \quad \text{with} \quad \rho_1 - \rho_2 = 0 \quad \text{(C12/m1)} \\ &\rho_1 + \rho_2 = 0 \quad \text{with} \quad \rho_1 - \rho_2 \neq 0 \quad \text{(C2/m11)} . \end{aligned} \tag{12}$$

The order parameter is then $\rho = 1/\sqrt{2}(\rho_1 \pm \rho_2)$ and :

$$\Delta\Phi_2 = A_2(T - T'_{c_2})\,\rho^2 + \left(C_2 + \frac{1}{2}D_2\right)\rho^4 + E_2\,\nu^2 + \frac{1}{2}F_2\,\rho^2\,\nu + \cdots . \tag{13}$$

4.1.3 *The* OHT ⇔ ORT *transition.* — The Pnam space-group of the ORT phase (or equivalently Pbnm) is a sub-group of the space-group Imam (Ibmm) of the OHT phase, resulting from a lattice instability occurring at point X $(0, 0, 2\pi/c_0)$ of the OHT Brillouin zone, driven by the X_4^-/B_{3u} representation. The order parameter μ for this transition is unidimensional, so that the free energy expansion has the classical form :

$$\Delta\Phi_3 = A_3(T - T_{c_1})\,\mu^2 + C_3\,\mu^4 + \cdots . \tag{14}$$

It should be noticed that point X in the OHT phase is issued from points $Z(0, 0, \pi/c_t)$ and $M(\pi/a_t, \pi/a_t, 0)$ of the THT Brillouin zone [32].

4.1.4 *The « family-tree » of* $2C_5Cd$. — In figure 13, we have represented the structural relationships existing between the different phases of $2C_5Cd$, deduced from the preceding discussion. Thus, the Imam (OHT phase) and Pnam (ORT phase) space-groups on the one hand, and the C12/m1 (MHT phase) space-group on the other hand belong to two different branches of sub-group issued from P4/mmm. The sequence THT ⇔ OHT ⇔ ORT may then correspond to two successive second-order phase transitions ; the OHT ⇔ ORT transition observed at T_{c_1} is indeed of second order. These is no group to sub-group relation between Imam and C12/m1, so that the transition OHT ⇔ MHT should be necessarily of first-order, which is in agreement with the experiments.

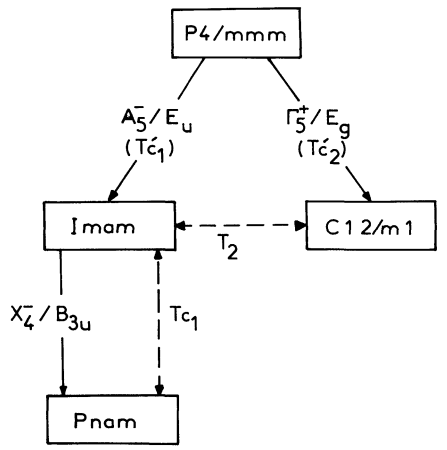

Fig. 13. — The « family-tree » of the different structural modifications of $2C_5Cd$. Full lines correspond to group sub-group relations, along with the symmetry properties of the primary order parameters. Broken lines correspond to the observed structural phase transitions.

4.2 THE MULTIDIMENSIONAL PSEUDO-SPIN MODEL. — The structural data obtained on the OHT phase of $2C_5Cd$ [18] have shown that orientational disorder of the chains can be described by a discrete set of equiprobable orientations between which the molecule jumps from time to time [19, 25] (Frenkel model). This means that a model of reorientable pseudo-spins attached to the molecule can be used to characterize the orientational disorder. However, in addition, one has to take account of the conformational disorder of the chains,

between « trans » and « twisted » states ; from relations (1) and (2), the conformational equilibrium is conveniently described by the following equation :

$$\frac{p}{(1-p)} = C \cdot \exp\left(\frac{-\Delta H}{RT}\right) \tag{15}$$

where C is a constant.

Let us first describe the structure of the fictitious THT phase in terms of a pseudo-spin model. The « trans » chains in the crystal of $2C_5Cd$ have the molecular C_{2v} symmetry, with the C_2 axis oriented at 45° from $\mathbf{a}_0$ and $\mathbf{b}_0$ [18], i.e. oriented along $\mathbf{a}_t$ or $\mathbf{b}_t$, and with one symmetry plane perpendicular to $\mathbf{c}_t$. Then, four energetically equivalent orientations of the « trans » chains are necessary to achieve statistically the D_{4h} site symmetry of the diammonium group in the THT phase (Fig. 14) :

$$\theta_1 = \theta_2 = \theta_3 = \theta_4 = \frac{1}{4}(1-p)\,. \tag{16}$$

The θ_i represent the probabilities of finding the « trans » chain in the orientation i. The idealized « twisted » chains have C_2 point symmetry [18], so that eight equiprobable orientations will statistically achieve the D_{4h} site symmetry (Fig. 14) :

$$\theta'_1 = \theta'_2 = \cdots = \theta'_8 = \frac{1}{8}p\,. \tag{17}$$

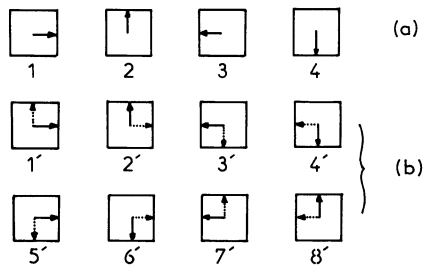

Fig. 14. — Schematic representation of orientational disorder of the pentylenediammonium chains in the parent phase (THT) of $2C_5Cd$. a) « trans » chains ; b) « twisted » chains.

Thus, we have to deal with a multidimensional pseudo-spin model, the theoretical processing of which is presented elsewhere [31] ; we shall give here only the main results of this treatment when applied to the case of $2C_5Cd$ (Tab. II). In a purely order-disorder description of the phase transitions, the order parameter components introduced in the free-energy expansions (relations (8), (11) and (14)) are identified to linear combinations of symmetrized coordinates Θ_j^α and $\Theta_j'^\alpha$ (j labels an irreducible representation and α labels a partner coordinate if the dimension of j is larger than one) constructed on the basis of the variables θ_i and θ'_i, respectively, with the help of projection operators [31]. These coordinates must be normalized respectively to $(1-p)$ and p, the proportions of « trans » and « twisted » chains.

Then, at $\mathbf{q} = 0$, four pseudo-spin coordinates Θ_j^α are found for the « trans » chains, with symmetries Γ_1^+/A_{1g}, Γ_3^+/B_{1g} and Γ_5^-/E_u, and eight coordinates $\Theta_j'^\alpha$ are associated with the « twisted » chains, with symmetries Γ_1^+/A_{1g}, Γ_4^+/B_{2g}, Γ_5^+/E_g, Γ_1^-/A_u, Γ_4^-/B_{2u} and

Table II. — *Description of the reorientational disorder of the pentylenediammonium chains in the different structural modifications of* $2C_5Cd$, *according to the multidimensional pseudo-spin model. See figure* 14 *for the label of the different orientations.*

Phase		"trans" chains	"twisted" chains
THT		$\bar{\theta}_1 = \bar{\theta}_2 = \bar{\theta}_3 = \bar{\theta}_4 = \frac{1}{4}(1-p)$	$\bar{\theta}'_1 = \bar{\theta}'_2 = \cdots = \bar{\theta}'_8 = \frac{1}{8}p$
MHT	$T<T'_{c_2}$	$\bar{\theta}_1 = \bar{\theta}_2 = \bar{\theta}_3 = \bar{\theta}_4 = \frac{1}{4}(1-p)$	$\bar{\theta}'_1 = \bar{\theta}'_4 > \bar{\theta}'_2 = \bar{\theta}'_3 > \bar{\theta}'_5 = \cdots = \bar{\theta}'_8$
	$T \ll T'_{c_2}$	$\bar{\theta}_1 = \bar{\theta}_2 = \bar{\theta}_3 = \bar{\theta}_4 = \frac{1}{4}(1-p)$	$\bar{\theta}'_1 = \bar{\theta}'_4 \approx \frac{1}{2}p, \bar{\theta}'_2 = \bar{\theta}'_3 \approx \bar{\theta}'_5 = \cdots = \bar{\theta}'_8 \approx 0$
OHT	$T<T'_{c_1}$	$\bar{\theta}_1 = \bar{\theta}_2 > \bar{\theta}_3 = \bar{\theta}_4$	$\bar{\theta}'_1 = \bar{\theta}'_2 > \bar{\theta}'_3 = \bar{\theta}'_4 > \bar{\theta}'_5 = \cdots = \bar{\theta}'_8$
	$T \ll T'_{c_1}$	$\bar{\theta}_1 = \bar{\theta}_2 \approx \frac{1}{2}(1-p), \bar{\theta}_3 = \bar{\theta}_4 \approx 0$	$\bar{\theta}'_1 = \bar{\theta}'_2 \approx \frac{1}{2}p, \bar{\theta}'_3 = \bar{\theta}'_4 \approx \bar{\theta}'_5 = \cdots = \bar{\theta}'_8 \approx 0$
ORT	$T<T_{c_1} \ll T'_{c_1}$	$\bar{\theta}_1 > \bar{\theta}_2, \bar{\theta}_3 \approx \bar{\theta}_4 \approx 0$	$\bar{\theta}'_1 = \bar{\theta}'_2 \approx \frac{1}{2}p, \bar{\theta}'_3 = \bar{\theta}'_4 \approx \bar{\theta}'_5 = \cdots = \bar{\theta}'_8 \approx 0$
	$T = 0$	$\bar{\theta}_1 = 1, \bar{\theta}_2 = \bar{\theta}_3 = \bar{\theta}_4 = 0$	$\bar{\theta}'_1 = \bar{\theta}'_2 = \cdots = \bar{\theta}'_8 = 0$

Γ_5^- / E_u. In the THT Brillouin zone, they generate four branches of pseudo-spin modes for the « trans » chains and eight branches for the « twisted » chains, issued from the different $\mathbf{q} = 0$ representations. All branches, excepted the A_{1g} ones, represent potential order parameters for the phase transitions [31].

4.2.1 *The* THT $\Leftrightarrow$ OHT $\Leftrightarrow$ ORT *phase sequence.* — The THT $\Leftrightarrow$ OHT transition is driven by a primary order parameter with A_5^- / E_u symmetry (Fig. 13), the representation Γ_4^+ / B_{2g} being associated with a secondary order parameter. The freezing of the relevant coordinates attached to the « trans » chains [31] induces a disordered state in OHT described by (Imam domains) :

$$\theta_1 = \theta_2 > \theta_3 = \theta_4 \quad \text{with} \quad \sum_i \theta_i = (1-p)\,. \tag{18}$$

Similarly, one obtains for the « twisted » chains [31] :

$$\theta'_1 = \theta'_2 > \theta'_3 = \theta'_4 > \theta'_5 = \theta'_6 = \theta'_7 = \theta'_8 \quad \text{with} \quad \sum_i \theta'_i = p\,. \tag{19}$$

At a finite temperature T such that $T \ll T'_{c_1}$ (Fig. 13), one gets approximately (Tab. II) :

$$\left.\begin{aligned} \theta_1 = \theta_2 &\approx \frac{1}{2}(1-p) \quad \text{with} \quad \theta_3 = \theta_4 \approx 0 \\ \theta'_1 = \theta'_2 &\approx \frac{1}{2}p \quad \text{with} \quad \theta'_3 = \cdots = \theta'_8 \approx 0\,. \end{aligned}\right\} \tag{20}$$

Relations (20) are in full agreement with the experimental data obtained at 353 K in the OHT phase [18], where both « trans » and « twisted » chains were found equally distributed between two mirror-related orientations, respectively (Fig. 14).

The OHT $\Leftrightarrow$ ORT transition is driven by an order parameter with X_4^- / B_{3u} symmetry

(Fig. 13). Then, the relevant coordinates of the « trans » chains which have not been frozen in the OHT phase [31], give for the ORT phase (Pnam domains) :

$$\left.\begin{array}{l} \theta_1 > \theta_2 > \theta_3 > \theta_4 \\ \text{or} \\ \theta_1 > \theta_2 > \theta_4 > \theta_3 \end{array}\right\} \quad \text{with } \sum_i \theta_i = (1-p)\,. \tag{21}$$

Similarly, one obtains for the « twisted » chains in the ORT phase :

$$\theta'_1 = \theta'_2 > \theta'_3 = \theta'_4 > \theta'_7 = \theta'_8 > \theta'_5 = \theta'_6 \quad \text{with } \sum_i \theta'_i = p\,. \tag{22}$$

At a finite temperature T such that $T \ll T_{c_1}$ (Fig. 13), one gets approximately (Tab. II) :

$$\left.\begin{array}{l} \theta_1 = (1-p) \quad \text{with } \theta_2 \approx \theta_3 \approx \theta_4 \approx 0 \\ \theta'_1 = \theta'_2 \approx \dfrac{1}{2}p \quad \text{with } \theta'_3 = \cdots = \theta'_8 \approx 0\,. \end{array}\right\} \tag{23}$$

According to relations (23), the residual disorder observed experimentally in the ORT phase at temperatures well below T_{c_1} (see Sect. 3.3 and 3.4.2) would be due essentially to the « twisted » chains which, in the ORT phase, remain in the same disordered state as in OHT {see relations (20) and (23)}. Indeed, the disordering mode (« Rayleigh wing ») observed on the B_{1_g} Raman spectrum tends to disappear around 200 K (Fig. 12), i.e. in the same temperature range where the « twisted » chains can no longer be observed in the region of the internal modes (Fig. 7).

Furthermore, if one considers the successive orientations of NH_3 ends along the crystallographical $\mathbf{c}_0$ direction (chain axis) in the ordered state, one has for the « trans » chains a sequence such as (1)-(1)...(2)-(2)...(1)-(1), etc... (see Fig. 14), due to the coupling of NH_3 orientations with octahedron « rotations » within the perovskite layers. So, the ordered phases of compounds with an odd number of carbon atoms and containing « trans » chains only will correspond necessarily to a lattice period along **c** equal to two inter-layer distances [6], as found in the ORT phase of $2C_5Cd$ [18] ; now, a hypothetical ordered state with « twisted » chains only would correspond to a sequence such as (1)-(2)...(1)-(2)...(1)-(2) etc..., i.e. where the lattice constant along **c** is equal to one inter-layer distance. In the hypothesis where disordering processes are due to, or are coupled to the disordered « twisted » chains, short range ordering along **c**, as evidenced in section 3.3.1, would give rise to the existence of domains characterized by a period of $c_0/2$. Indeed, the short modulation of the diffuse streaks (Fig. 4) corresponds to diffuse spots with even values of the index ℓ, as expected for a period of $c_0/2$ that would be effective in a short range.

Finally, we emphasize that the ORT ground state (obtained at $T = 0$) is completely ordered, with « trans » chains only : as deduced from relations (15), (21) and (22), one finds $\theta_1 = 1$ with all other $\theta_i = 0$ and $\theta'_i = 0$. Again, this is in full agreement with the experimental data.

4.2.2 *The* THT $\Leftrightarrow$ MHT *transition.* — The fictitious THT $\Leftrightarrow$ MHT transition is driven by the Γ_5^+/E_g irreducible representation of the P4/mmm space-group (Fig. 13), Γ_4^+/B_{2g} acting as a secondary order parameter. None of the pseudo-spin coordinates attached to the « trans » chains correspond to these representations, so that the « trans » chains in MHT must stay in the same disordered state as in THT, i.e. (Tab. II) :

$$\theta_1 = \theta_2 = \theta_3 = \theta_4 = \frac{1}{4}(1-p)\,. \tag{24}$$

In contrast, there are three relevant coordinates related to the « twisted » chains [31] which give :

$$\theta'_1 = \theta'_4 > \theta'_2 = \theta'_3 > \theta'_5 = \theta'_6 = \theta'_7 = \theta'_8 \quad \text{with} \quad \sum_i \theta'_i = p \,. \tag{25}$$

From relations (24) and (25), it is clear that the MHT ground state cannot be ordered, so that a phase transition at $T < T'_{c_2}$ (Fig. 13) is necessary to obtain an ordered state at $T = 0$. Furthermore, the equilibrium value of the order parameter (Eq. (13)) :

$$\rho_0 = \theta'_1 - \frac{1}{2}(\theta'_2 + \theta'_5)$$

is always proportional to p. This means that $\rho_0 \Rightarrow 0$ when $T \Rightarrow 0$ (Eq. (15)) ; in other words, the MHT phase is stabilized by the presence of « twisted » chains.

At a finite temperature T such that $T \ll T'_{c_2}$ (Fig. 13), relation (24) is still valid, but one gets from (25) (Tab. II) :

$$\theta'_1 = \theta'_4 \approx \frac{1}{2}p, \quad \text{with} \quad \theta'_2 = \theta'_3 \approx \theta'_5 = \cdots = \theta'_8 \approx 0 \,. \tag{26}$$

4.2.3 *The* MHT $\Leftrightarrow$ OHT *transition.* — The MHT $\Leftrightarrow$ OHT transition corresponds to a shift from one branch of the sub-group to another one (Fig. 13). Such a behaviour is well known in systems with competing order-parameters. The competing interactions in $2C_5Cd$ are due to the « trans » $\Leftrightarrow$ « twisted » equilibrium. As shown previously, increasing values of p with increasing temperature is a stabilizing factor for the MHT phase ; so, as long as p is sufficiently low, the OHT (or ORT) phase is stable, while, above a threshold value of p attained at T_2, the MHT phase becomes stable through a first order phase transition : at $T > T_2$, the minimum in ρ of $\Delta\Phi_2$ (Eq. (13)) becomes deeper than the minimum in η of $\Delta\Phi_1$ (Eq. (10)).

As this point, it is worth noting that a Boltzmann distribution between « trans » and « twisted » states of the chains as described by equation (15) is only valid if the coupling energy to the octahedron sub-lattice does not vary strongly with temperature, in particular at the phase transitions, and if the single particle energy difference between these two states (governed by the internal potential of the chain) strongly dominates over the two-particle interaction energies (« trans »-« trans », « twisted »-« twisted » and « trans »-« twisted ») appearing in the free-energy expansion [6, 31]. Apparently, these conditions hold true in the temperature range of stability of the OHT and ORT phases (Fig. 8), but of course equation (15) is unable to account for the shift of the « trans » $\Leftrightarrow$ « twisted » equilibrium in favour of « twisted » chains observed at the OHT $\Leftrightarrow$ MHT transition occurring at $T_2 = 417$ K (see Figs. 3 and 7). Indeed, the OHT $\Leftrightarrow$ ORT phase transition is non-ferroelastic, so that only the volume strain is expected to vary with temperature (see Sect. 3.2.1), whereas a very strong shear deformation takes place in the MHT phase (Fig. 3). Then, a full proportion of « twisted » chains in MHT could be explained by a coupling with the octahedron sub-lattice, if this conformation fits better the distorted MHT network than the « trans » ones.

On the other hand, the configurational entropy excess in the MHT ground state with $p = 1$ (see relation (26)) would be $S_{ex}^{(MHT)} = R \,\mathrm{Ln}\, 2$. Also, according to the experimental results, the disordered OHT state is well described by relations (20) derived from the conditions $T_{c_1} < T_2 \ll T'_{c_1}$ (Fig. 13), which means that $R \,\mathrm{Ln}\, 2 < S_{ex}^{(OHT)} \leqq R \,\mathrm{Ln}\, 4$, depending on the value of p ($0 < p \leqq 0.5$, (see Sect. 3.4.3)). Since at T_2 one should have $S_{ex}^{(MHT)} \geqq S_{ex}^{(OHT)}$,

relation (26) derived for $T \ll T'_{c_2}$ is not appropriate to describe the orientational disorder in the MHT phase just above T_2, but one has more likely to consider relation (25) corresponding to higher relative temperatures, and allowing higher values of $S_{ex}^{(MHT)}$, namely $R \text{ Ln } 2 < S_{ex}^{(MHT)} \leqq R \text{ Ln } 8$ (with $p = 1$). In other words, according to this model, the MHT phase is far from being in its ground state at the transition temperature T_2 and the approximation $T_2 \ll T'_{c_2}$ (Tab. II) is not valid.

There is however another possibility to achieve a disordered MHT structure with « twisted » chains only, which consists in a rotation by $\approx 45°$ of the NH_3 equilibrium positions in the $(\mathbf{a}_m \mathbf{b}_m)$ plane ; a similar change of the hydrogen bonding scheme has been reported for the « trans » chains in $2C_3Mn$, taking place in a narrow range of temperature [15, 25, 29]. Then, the THT parent phase still corresponds to a distribution between eight equiprobable orientations of such « twisted » chains, but for symmetry reasons, the MHT ground state now corresponds to a distribution between four equivalent orientations. According to this model, one always has $S_{ex}^{(MHT)} \geqq R \text{ Ln } 4 \geqq S_{ex}^{(OHT)}$, even though the MHT ground state is almost achieved at T_2. Thus, the OHT $\Leftrightarrow$ MHT transition would correspond to a change in the NH_3 hydrogen bonding schemes, in addition to the shift of the « trans » $\Leftrightarrow$ « twisted » equilibrium in favour of the « twisted » chains. Unfortunately, the experimental results up to now available do not allow us to make a choice between these two models proposed for the MHT phase.

5. Conclusions.

The experimental study of the structural phase transitions occurring in $2C_5Cd$ has shown the existence of complex phenomena due to the superposition of orientational and conformational disorders of the pentylenediammonium chains. A model of multidimensional pseudo-spins attached to the chain orientations is able to account for the unusual phase sequence of this material.

The conformational disorder is described by an equilibrium reaction of the chain between « trans » and « twisted » conformations. The thermally activated « twisted » states of the chains correspond to a conformation where one NH_3 end of the diammonium group is rotated by $\approx 90°$ with respect to the other one, and with a constant twist angle along the chain between two neighbouring carbon atoms.

The OHT $\Leftrightarrow$ ORT phase transition observed at $T_{c_1} = 337$ K is due to the orientational ordering of the « trans » chains, whereas the « twisted » chains remain orientationally disordered in both phases ; on the other hand, the « trans » $\Leftrightarrow$ « twisted » equilibrium is apparently not modified by this transition. The ORT phase progressively gets ordered at low temperatures, as a result of the disappearance of the « twisted » chains by thermal effect. Thus, the residual disorder observed in ORT well below T_{c_1} is assigned to the presence of disordered « twisted » chains ; the coupling of reorientational motions of these chains to the octahedron sub-lattice gives rise to the existence of short range ordering phenomena, responsible for the observation of diffuse X-ray scattering patterns and of peculiar features (« Rayleigh wing » signal) in the Raman spectra.

The OHT $\Leftrightarrow$ MHT phase transition observed at $T_2 = 417$ K occurs when the proportion p of « twisted » chains has reached a threshold value. The MHT structure is strongly distorted and favours the « twisted » chains ; the MHT phase containing only « twisted » chains is also shown to be orientationally disordered.

Acknowledgments.

The authors wish to thank Drs. C. Sourisseau and F. Guillaume (Laboratoire de Spectroscopie Moléculaire et Cristalline, Université de Bordeaux I) for helpful discussions and for communication of their neutron scattering results prior to publication. It is also a pleasure to acknowledge Professor R. M. Pick and Dr. H. Poulet (Département de Recherches Physiques, Université de Pàriv VI) for a general formulation of the multidimensional pseudospin model [31].

References

[1] KIND, R., *Ferroelectrics* **24** (1980) 81.
[2] MOKHLISSE, R., COUZI, M., CHANH, N. B., HAGET, Y., HAUW, C. and MERESSE, A., *J. Phys. Chem. Solids* **46** (1985) 187.
[3] CHANH, N. B., HAUW, C., MERESSE, A., REY-LAFON, M. and RICARD, L. *J. Phys. Chem. Solids* **46** (1985) 1413.
[4] WHITE, M. A., *J. Chem. Phys.* **81** (1984) 6100.
[5] HAGEMANN, H. and BILL, H., *J. Phys. C: Solid State Phys.* **18** (1985) 6441.
[6] KIND, R., PLESKO, S., GUNTER, P., ROOS, J. and FOUSEK, J., *Phys. Rev. B* **23** (1981) 5301 and *B* **24** (1981) 4910.
[7] BIRELL, G. B. and ZASLOW B., *J. Inorg. Nucl. Chem.* **34** (1972) 1751.
[8] WILLETT, R. D. and RIEDEL, E. F., *Chem. Phys.* **8** (1975) 112.
[9] WILLETT, R. D., *Acta Cryst.* **B 33** (1977) 1641.
[10] TICHY, K., BENES, J., HALG, W. and AREND, H., *Acta Cryst.* **B 34** (1978) 2970.
[11] TICHY, K., BENES, J., KIND, R. and AREND, H., *Acta Cryst.* **B 36** (1980) 1355.
[12] CROWLEY, J. C., DODGEN, H. W. and WILLETT, R. D., *J. Phys. Chem.* **86** (1982) 4046.
[13] LEVSTIK, A., FILIPIC, C., BLINC, R., AREND, H. and KIND, R., *Solid State Commun.* **20** (1976) 127.
[14] BLINC, R., BURGAR, M., LOZAR, B., SELIGER, J., SLAK, J., RUTAR, V., AREND, H. and KIND, R., *J. Chem. Phys.* **66** (1977) 278.
[15] KIND, R., PLESKO, S. and ROOS, J., *Phys. Stat. Solidi* **47(a)** (1978) 233.
[16] FOUSKOVA, A., *Ferroelectrics* **25** (1980) 451.
[17] NEGRIER, P., COUZI, M., CHANH, N. B., HAUW, C. and MERESSE, A., Dynamics of Molecular Crystals, Ed. Lascombe, J. (Elsevier Science Pub.) Amsterdam (1987) p. 231.
[18] NEGRIER, P., CHANH, N. B., COURSEILLE, C., HAUW, C., MERESSE, A. and COUZI, M., *Phys. Stat. Solidi* **100 (a)** (1987) 473.
[19] GUILLAUME, F., SOURISSEAU, C., LUCAZEAU, G. and DIANOUX, A. J., Dynamics of Molecular Crystals Ed. Lascombe J. (Elsevier Science Pub.) Amsterdam (1987) p. 173.
[20] MOKHLISSE, R., CHANH, N. B., COUZI, M., HAGET, Y., HAUW, C. and MERESSE, A., *J. Phys. C: Solid State Phys.* **17** (1984) 233.
[21] DENOYER, F., COMES, R., LAMBERT, M. and GUINIER, A., *Acta Cryst.* **A 30** (1974) 423.
[22] NEGRIER, P., Thesis, University of Bordeaux I, (1987).
[23] COUZI, M. and NEGRIER, P., unpublished results.
[24] MAISSARA, M., CORNUT, J. C., DEVAURE, J. and LASCOMBE, J., *Spectrosc. Int. J.* **2** (1983) 104.
[25] GUILLAUME, F., SOURISSEAU, C., LUCAZEAU, G. and DIANOUX, A. J., *Mol. Phys.* **58** (1986) 413.
[26] CHHOR, K., ABELLO, L., POMMIER, C. and SOURISSEAU, C., *J. Phys. Chem. Solids* **49** (1988) 1079.
[27] MOKHLISSE, R., COUZI, M. and LASSEGUES, J. C., *J. Phys. C: Solid State Phys.* **16** (1983) 1353.
[28] MOKHLISSE, R., COUZI, M. and LOYZANCE, P. L., *J. Phys. C: Solid State Phys.* **16** (1983) 1367.
[29] SOURISSEAU, C. and LUCAZEAU, G., *J. Raman Spectrosc.* **8** (1979) 391.

[30] POULET, H. and MATHIEU, J. P., Spectres de vibration et symétrie des cristaux (Gordon and Breach) Paris (1970).
[31] COUZI, M., NEGRIER, P., POULET, H. and PICK, R. M., *Croat. Chem. Acta* (in press).
[32] BRADLEY, C. J. and CRACKNELL, A. P., The Mathematical theory of symmetry in solids (Clarendon Press) Oxford (1972).